


Cite this: *RSC Adv.*, 2019, 9, 3337

# Acetylacetone functionalized magnetic carbon microspheres for the highly-efficient adsorption of heavy metal ions from aqueous solutions

Jie Ma, \* Mengya Sun, Yulan Zeng, Zhenhua Liu, Manman Zhang, Yao Xiao and Shuping Zhang

Herein, Acac-C@Fe<sub>3</sub>O<sub>4</sub>, a magnetic carbon (C@Fe<sub>3</sub>O<sub>4</sub>) modified with acetylacetone (Acac), was first prepared and used as a solid-phase adsorbent for adsorbing some heavy metal ions from aqueous solution. The adsorbent was characterized by Fourier transform infrared spectroscopy (FTIR), X-ray diffraction (XRD), scanning electron microscopy (SEM), transmission electron microscopy (TEM), X-ray photoelectron spectroscopy (XPS), vibrating sample magnetometry (VSM) and BET studies. Some parameters affecting the adsorption and desorption processes were studied in Pb<sup>2+</sup> solution, including sample pH, contact time, initial concentration, type and connection of the desorption solution. Adsorption results showed that removal of Pb<sup>2+</sup> was 100% under optimal conditions at an initial concentration of 10.0 mg L<sup>-1</sup>. The adsorption mechanism conformed well to a pseudo-second order kinetic model. The adsorption capacity of the sorbent also showed promising results with Hg<sup>2+</sup>, Cr<sup>3+</sup>, Fe<sup>2+</sup>, Cd<sup>2+</sup>, Mn<sup>2+</sup>, Zn<sup>2+</sup>, Cu<sup>2+</sup> and Pb<sup>2+</sup>, where maximum adsorption capacities reached 98.0, 151.2, 188.9, 202.2, 286.3, 297.2, 305.1 and 345.3 mg g<sup>-1</sup>, respectively. The Acac-C@Fe<sub>3</sub>O<sub>4</sub> microsphere material was successfully applied to the adsorption of heavy metal ions in aqueous solution.

Received 29th November 2018  
Accepted 11th January 2019

DOI: 10.1039/c8ra09830a

rsc.li/rsc-advances

## Introduction

With the growth of industrial activities, the phenomenon of highly toxic heavy metal ions release to water resources becomes more and more serious.<sup>1</sup> Heavy metals are difficult to biodegrade and can be enriched hundreds of times during biological amplification of the food chain before entering the human body. Eventually, they will make proteins and enzymes inactive and also cause chronic poisoning.<sup>2</sup> Thus, it becomes even more necessary to establish a facile and reliable method to deal with environmental pollution of heavy metal ions. Over decades, several technologies have been developed to remove heavy metal ions from wastewaters such as chemical precipitation (including hydroxide precipitation,<sup>3</sup> sulphide precipitation<sup>4</sup> and chelating precipitation<sup>5</sup>), ion exchange,<sup>6</sup> membrane filtration (including ultrafiltration,<sup>7</sup> reverse osmosis and nanofiltration<sup>8</sup> and electrodialysis<sup>9</sup>), coagulation and flocculation,<sup>10</sup> flotation,<sup>11</sup> electrochemical treatment<sup>12</sup> and adsorption.<sup>13</sup> Adsorption methods draw more attention, because they are simple to pursue without additional consumption, high performing and cost-effective.

With all of the absorbing materials, magnetic nanomaterials are different from others as they can be collected by external

magnetic fields.<sup>14</sup> This performance provides both adsorption and desorption post-processing for convenience. Meanwhile, low-cost nanosized ferric oxides (Fe<sub>3</sub>O<sub>4</sub> or γ-Fe<sub>2</sub>O<sub>3</sub>) possess non-toxicity and superparamagnetism and therefore they have gained even more interest.<sup>15</sup> Aggregation of these particles can be regulated and controlled by a surface modified process and so far abundant materials have been used as a modified layer including silicon, carbon, synthetic polymers and metals. Among these materials, carbon-based materials are popularly selected because they are easily synthesized and eco-friendly, especially when they have numerous hydrophilic groups and can provide favourable conditions for further modification.<sup>16</sup> Wang *et al.* prepared two different structures of carbon-coated Fe<sub>3</sub>O<sub>4</sub> for lithium storage; both composite materials have good performance and represent a good future for applications. There are also many applications of Fe<sub>3</sub>O<sub>4</sub>@C nanomaterials in the environmental treatment fields.<sup>17</sup> Liu *et al.* designed 1D Fe<sub>3</sub>O<sub>4</sub>/C/CdS coaxial nanochains for the degradation of RhB.<sup>18</sup> Bystrzejewski *et al.* prepared carbon-encapsulated magnetic nanoparticles to adsorb Cu<sup>2+</sup>, Co<sup>2+</sup>, and Cd<sup>2+</sup> and their adsorption capacities were 3.21, 1.23 and 1.77 mg g<sup>-1</sup>, respectively.<sup>19</sup> Chen *et al.* synthesized magnetic core-shell Fe<sub>3</sub>O<sub>4</sub>@C nanoparticles with -SO<sub>3</sub>H/-COOH groups modified for adsorbing Pb<sup>2+</sup>, Hg<sup>2+</sup> and Cd<sup>2+</sup> ions and their maximum adsorptions were 90.7, 83.1 and 39.7 mg g<sup>-1</sup>, respectively.<sup>20</sup> The above-mentioned carbon coated magnetic nanomaterials could be used to adsorb heavy metal ions, but their absorption

College of Science, University of Shanghai for Science and Technology, Shanghai 200093, P. R. China. E-mail: majie0203ch@hotmail.com; Fax: +86 21 55271663; Tel: +86-13482433498

capacities are limited, which may be improved by some new methods.

In order to improve adsorption properties of adsorbents, some chelate molecules, especially multidentate ligands, were selected to modify nanomaterials, such as ethylene diamine tetraacetic acid (EDTA), ethanediamine (EDA) and acetylacetone (Acac), which showed strong coordination with metal ions. Among them, the Acac molecules are superior to other molecules because their active hydrogen and the dicarbonyl structures can be retained during the modification process.<sup>21</sup> In this work, the magnetic carbon composite (C@Fe<sub>3</sub>O<sub>4</sub>) was synthesized by a hydrothermal method and functionalized with Acac for adsorbing heavy metal ions in an aqueous solution. Behaviours of the adsorption in different analytical conditions and performance under optimized conditions were investigated by FAAS determination. Meanwhile, the adsorption capacities of the as-prepared composites for Cu<sup>2+</sup>, Zn<sup>2+</sup>, Mn<sup>2+</sup>, Cd<sup>2+</sup>, Fe<sup>2+</sup>, Hg<sup>2+</sup> and Cr<sup>3+</sup> were measured and had ideal results. Thus the Acac modified C@Fe<sub>3</sub>O<sub>4</sub> microspheres (Acac-C@Fe<sub>3</sub>O<sub>4</sub>) may be used in the metal ion wastewater treatment.

## Experimental

### Materials

All reagents were of analytical grade including FeCl<sub>3</sub>·6H<sub>2</sub>O, Pb(NO<sub>3</sub>)<sub>2</sub>·6H<sub>2</sub>O, FeSO<sub>4</sub>·7H<sub>2</sub>O, CuSO<sub>4</sub>·5H<sub>2</sub>O, ZnCl<sub>2</sub>, HgCl<sub>2</sub>, CrCl<sub>3</sub>·6H<sub>2</sub>O, MnSO<sub>4</sub>, CdCl<sub>2</sub>·2.5H<sub>2</sub>O, NaOH, CH<sub>3</sub>COONa, ethylene glycol (C<sub>2</sub>H<sub>6</sub>O<sub>2</sub>), D(+)-glucose monohydrate (C<sub>6</sub>H<sub>12</sub>O<sub>6</sub>·H<sub>2</sub>O), ethanediamine (C<sub>2</sub>H<sub>8</sub>O<sub>2</sub>), (3-chloropropyl)triethoxysilane (C<sub>9</sub>H<sub>21</sub>ClO<sub>3</sub>Si, KH230), acetylacetone (Acac), and HCl solution and all were purchased from Sinopharm Chemical Reagent Corporation (Shanghai, China). A target stock solution of Pb<sup>2+</sup> with 1000.0 mg L<sup>-1</sup> was prepared by dissolving proper amounts of Pb(NO<sub>3</sub>)<sub>2</sub>·6H<sub>2</sub>O and nitric acid in distilled water. Then the solution was further diluted to the given concentrations for testing adsorption capacity and analysing the pre-concentration process.

### Instrumentation

The morphology of a sorbent was detected by a field emission scanning electron microscope (SEM, VEGA3 TESCAN, CZ) and a transmission electron microscope (TEM, H800EM Hitachi, JP). Surface area was measured by a BET instrument (TriStar 3020 Micromeritics, CN). XPS spectra were measured by an X-ray photoelectron spectroscope (XPS, Thermo ESCALAB 250XI, CN). A Fourier transform infrared spectrophotometry analysis was performed using a FTIR spectrophotometer (FTIR, Nicolet, USA) equipped with a KBr beam splitter. X-ray diffraction patterns of the samples were recorded by an X-ray powder diffractometer (XRD, D8 advance, DE). Magnetic properties of the sorbent were tested using a vibrating sample magnetometer (VSM, EZ-VSM, MicroSense, USA) at room temperature. Concentrations of metal ions were measured using a flame atomic absorption spectrophotometer with air-acetylene (FAAS, TAS990, China). A digital pH meter was used for pH adjustment of the solutions.

### Preparation of Acac-C@Fe<sub>3</sub>O<sub>4</sub>

The synthetic process is shown in Scheme 1. First, a solvothermal method was adopted for synthesizing Fe<sub>3</sub>O<sub>4</sub> magnetic composites according to a previously reported procedure.<sup>22</sup> In a typical procedure, 36 mmol of FeCl<sub>3</sub>·6H<sub>2</sub>O and 200 mmol of CH<sub>3</sub>COONa were dissolved in 350.0 mL ethylene glycol. The mixture was sonicated for 30 min and then stirred at room temperature for 2 h. Afterward, the homogeneous solution was transferred into a 500 mL Teflon-lined stainless-steel autoclave and reacted at 200 °C for 10 h followed by cooling down to room temperature naturally. The product was washed with ethanol and distilled water for several times, and then dried in a vacuum freeze-drying apparatus for 5 h.

Secondly, C@Fe<sub>3</sub>O<sub>4</sub> was prepared by a facile hydrothermal method.<sup>23,24</sup> Concretely, 0.5 g Fe<sub>3</sub>O<sub>4</sub> nanoparticles were dispersed in 0.1 mol L<sup>-1</sup> HNO<sub>3</sub> solution and sonicated for 10 min, then were rinsed with distilled water several times until neutral. Subsequently, 8.2 g glucose was dissolved in 80.0 mL distilled water, followed by the addition of 0.5 g Fe<sub>3</sub>O<sub>4</sub> under sonication. The pH value of the mixture was adjusted to 8.0 by a 0.1 mol L<sup>-1</sup> NaOH solution. Afterwards, the mixture solution was transferred into a Teflon-lined stainless-steel autoclave (100 mL capacity) and heated at 170 °C for 4 h. The precipitate was washed with distilled water for several times and dried in a vacuum freeze-drying apparatus for 5 h, and then the carbon coated Fe<sub>3</sub>O<sub>4</sub> nanomaterials were obtained.

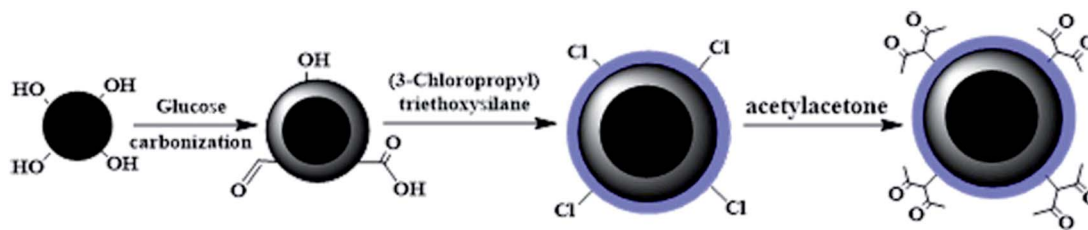
Thirdly, 1.0 g C@Fe<sub>3</sub>O<sub>4</sub> was dissolved in 100.0 mL water-ethanol under mechanical stirring. Then, 1.0 mL ammonia (25%) and 3.0 mL KH230 were added dropwise to the reaction mixture under constant stirring at 45 °C. After 1 h, the reaction mixture was heated to 60 °C and stirred constantly for 1 h, and then cooled to room temperature. Finally, the magnetic samples (KH230-C@Fe<sub>3</sub>O<sub>4</sub>) were isolated by using an external magnet, washed thoroughly with distilled water and ethanol several times, and then dried in a vacuum freeze-drying apparatus.

Finally, 1.0 g NaOH was dissolved in 10.0 mL distilled water and then was added to 40.0 mL ethanol in an ice-water bath, 10.0 mL Acac was added into the mixture, followed by 1.0 g KH230-C@Fe<sub>3</sub>O<sub>4</sub> which was dispersed into the suspension under constant stirring for 0.5 h. Then the mixture was heated to 33 °C for 7 h. The sample was separated using an external magnetic field and washed several times with distilled water and ethanol and dried in a vacuum freeze-drying apparatus. Finally, Acac-C@Fe<sub>3</sub>O<sub>4</sub> composites were prepared successfully.

### Adsorption procedure

Aqueous solutions with different Pb<sup>2+</sup> concentrations were prepared and adjusted to a given pH value by HCl and NaOH, and then 5.0 mg sorbent was dispersed into the above solution (25.0 mL). The time dependence of the adsorption capacity was also examined as a function of contact time from 1 to 8 min at room temperature using 25.0 mL of Pb<sup>2+</sup> solution (20.0 mg g<sup>-1</sup>) mixed with 5.0 mg of sorbent. The Pb<sup>2+</sup> concentration of a sample was measured by FAAS. The adsorption capacity of the material for Cu<sup>2+</sup>, Zn<sup>2+</sup>, Mn<sup>2+</sup>, Cd<sup>2+</sup>, Fe<sup>2+</sup>, Hg<sup>2+</sup> and Cr<sup>3+</sup> were researched under the same conditions. The adsorption process is shown in Fig. 1.





Scheme 1 Diagram of the Acac-C@Fe<sub>3</sub>O<sub>4</sub> magnetic material synthesis process.

## Result and discussion

### Characterization of the magnetic microspheres

**VSM analysis.** Fig. 2a depicts the magnetization hysteresis loops of typical samples including Fe<sub>3</sub>O<sub>4</sub>, C@Fe<sub>3</sub>O<sub>4</sub> and Acac-C@Fe<sub>3</sub>O<sub>4</sub> microspheres at room temperature. The curves indicated that all prepared samples had superparamagnetic properties with negligible magnetic remanence and coercivity. Saturation magnetization of samples decreased from 30 to 14 emu g<sup>-1</sup> with an increase of coating layer which showed that the obtained samples had enough magnetic response characteristics to meet magnetic separation process.

Meanwhile, the coercivities of samples were almost stable below 20 Oe. The above suggested the modified layer did not affect the superparamagnetic feature of the composites, but just reduced the saturation magnetization of a sample due to the decreased content of Fe<sub>3</sub>O<sub>4</sub> component in the microspheres.

**X-ray diffraction analysis.** The XRD patterns of Fe<sub>3</sub>O<sub>4</sub>, C@Fe<sub>3</sub>O<sub>4</sub> and Acac-C@Fe<sub>3</sub>O<sub>4</sub> magnetic particles are presented in Fig. 2b. The similar diffraction peaks of all patterns, including 30.1°, 35.5°, 43.0°, 53.6°, 57.0° and 62.6°, indicated the crystal structures of all composites were coincided with a Fe<sub>3</sub>O<sub>4</sub> standard specimen as a cubic spinel structure (JCPDS, no. 19-0629).<sup>25</sup> The X-ray diffraction patterns of C@Fe<sub>3</sub>O<sub>4</sub> and Acac-C@Fe<sub>3</sub>O<sub>4</sub> were similar with the pattern of Fe<sub>3</sub>O<sub>4</sub> magnetic particles, which illuminated that they had the same crystal structure and it was not changed during the modification procedures.

**FTIR analysis.** Composition of the Acac-C@Fe<sub>3</sub>O<sub>4</sub> composite was further characterized by FT-IR spectrophotometry, and the relevant results are shown in Fig. 2c. The specific stretching vibration absorption peak of Fe–O in Fe<sub>3</sub>O<sub>4</sub> was obviously visible in four spectra at 586 cm<sup>-1</sup>, which indicated all samples

contained Fe<sub>3</sub>O<sub>4</sub>. The peaks at 1623 cm<sup>-1</sup> and 1689 cm<sup>-1</sup> were attributed to C=C and C=O vibrations and illustrated that carbon was successfully coated on the magnetic core. Meanwhile the absorption peak at 3434 cm<sup>-1</sup> implied the existence of residual hydroxyl groups, which confirmed that some hydrophilic groups (–OH) and carbonyl group (–C=O) remained after the process of hydrothermal carbonization treatment.<sup>26–28</sup> The peak at 802 cm<sup>-1</sup> shown in Fig. 2c indicated the existence of C–Cl groups and suggested that KH230 were grafted on the surface of C@Fe<sub>3</sub>O<sub>4</sub> composites. Curves of Acac-C@Fe<sub>3</sub>O<sub>4</sub>, KH230-C@Fe<sub>3</sub>O<sub>4</sub> and Fe<sub>3</sub>O<sub>4</sub> are compared and shown in Fig. 2c and the enhancement of a peak at 1623 cm<sup>-1</sup> is attributed to the carbonyl stretching vibration<sup>29</sup> while the peak at 2915 cm<sup>-1</sup> indicated the existence of –CH<sub>3</sub> of Acac. These FTIR data indicated that Acac successfully functionalized the C@Fe<sub>3</sub>O<sub>4</sub> magnetic microspheres.

**BET analysis.** The ratio surface areas of Fe<sub>3</sub>O<sub>4</sub> and Acac-C@Fe<sub>3</sub>O<sub>4</sub> were analysed by nitrogen adsorption–desorption techniques. As Fig. 2d shows, the nitrogen adsorption–desorption isotherms of Fe<sub>3</sub>O<sub>4</sub> and Acac-C@Fe<sub>3</sub>O<sub>4</sub> have representative type-IV curves. The hysteric loop in the range of 0.6–0.9 *P/P*<sub>0</sub> is a type of H1 hysteresis. The BET specific surface area of Acac-C@Fe<sub>3</sub>O<sub>4</sub> was measured to be 68.41 m<sup>2</sup> g<sup>-1</sup>, which is higher than that of Fe<sub>3</sub>O<sub>4</sub> (37.41 m<sup>2</sup> g<sup>-1</sup>). This change might be

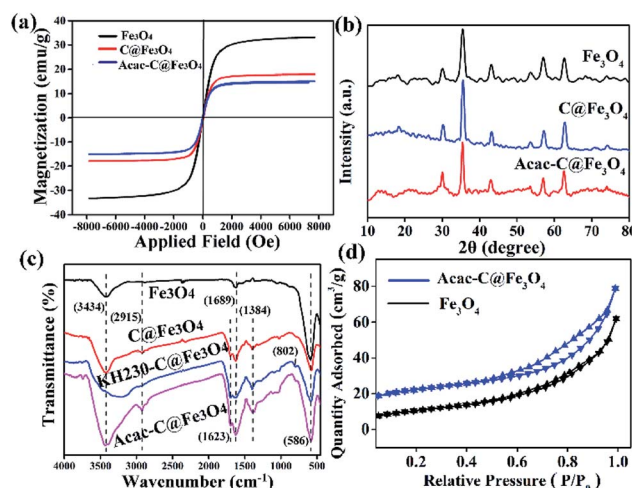


Fig. 2 (a) Magnetization curves of typical prepared samples: Fe<sub>3</sub>O<sub>4</sub>, C@Fe<sub>3</sub>O<sub>4</sub> and Acac-C@Fe<sub>3</sub>O<sub>4</sub>. (b) XRD patterns of Fe<sub>3</sub>O<sub>4</sub>, C@Fe<sub>3</sub>O<sub>4</sub> and Acac-C@Fe<sub>3</sub>O<sub>4</sub>. (c) FT-IR spectra of Fe<sub>3</sub>O<sub>4</sub>, C@Fe<sub>3</sub>O<sub>4</sub>, KH230-C@Fe<sub>3</sub>O<sub>4</sub> and Acac-C@Fe<sub>3</sub>O<sub>4</sub>. (d) Nitrogen adsorption–desorption isotherm of Fe<sub>3</sub>O<sub>4</sub> and Acac-C@Fe<sub>3</sub>O<sub>4</sub>.



Fig. 1 Schematic diagram of the adsorption process.





attributed to the porous structure of Acac-C@Fe<sub>3</sub>O<sub>4</sub> coming from carbon coating.

**XPS analysis.** The surface element composition of Acac-C@Fe<sub>3</sub>O<sub>4</sub> was determined by XPS spectra. As shown in Fig. 3a, the elements of Fe, C, O, and Si were detected on the surfaces of the nanocomposites. The signals of Fe and Si were weaker than that of C, indicating that the Fe<sub>3</sub>O<sub>4</sub> core is coated completely by the carbon shell and a small amount of KH230 was modified. The high-resolution XPS spectrum of Fe 2p can be fitted into two main doublet peaks, as shown in Fig. 3b. In the high-resolution spectrum, it can be seen that the doublet peak at 710.8 eV and 724.2 eV are assigned to Fe 2p<sub>3/2</sub> and Fe 2p<sub>1/2</sub>, which can be attributed to Fe(II) and Fe(III) of the Fe<sub>3</sub>O<sub>4</sub> core. These results were consistent with the XRD analysis. In Fig. 3c, there are more than one chemical state of C in the C 1s region; there peaks were identified and assigned to C-C and C-H (284.8 eV), C-O (286.5 eV), and C=O species (288.4 eV), respectively. These may be ascribed to a carbon shell and acetylacetone.<sup>30</sup> The XRD results and previous conclusions were combined and provide supportive evidence for the successful modification of carbon and Acac.

**SEM and TEM analysis.** Morphology and structures of the Fe<sub>3</sub>O<sub>4</sub>, C@Fe<sub>3</sub>O<sub>4</sub> and Acac-C@Fe<sub>3</sub>O<sub>4</sub> microspheres were characterized by scanning electron microscopy and transmission electron microscopy. Fig. 4 indicated the as-prepared Fe<sub>3</sub>O<sub>4</sub> materials were monodispersed microspheres, which were further proved by the relative TEM image of Fe<sub>3</sub>O<sub>4</sub> shown in Fig. 5. The average size of a microsphere is about 260 nm. Fig. 4 also confirmed that the Acac-C@Fe<sub>3</sub>O<sub>4</sub> sample still kept spherical morphology with a broader size distribution. The particle distribution range increased slightly, and the average of size of a microsphere increased to 400 nm. The increase of particle sizes and edges of C@Fe<sub>3</sub>O<sub>4</sub> and Acac-C@Fe<sub>3</sub>O<sub>4</sub> looked like a light shadow layer should be attributed to the carbon coating on the surface of the magnetic core, which was confirmed directly by the TEM image in Fig. 5. This further indicated that the Acac-C@Fe<sub>3</sub>O<sub>4</sub> composite was prepared successfully.

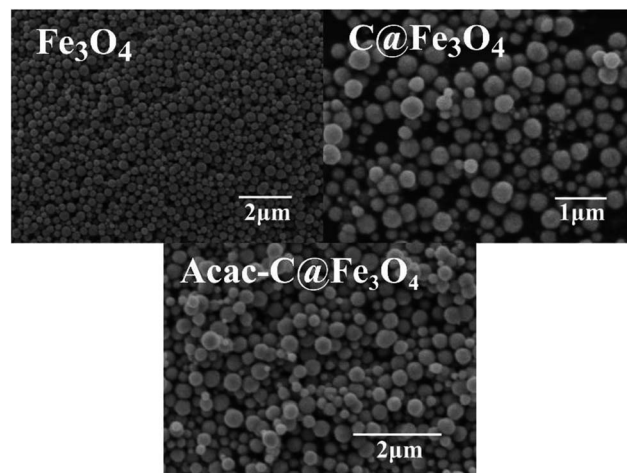


Fig. 4 SEM images of Fe<sub>3</sub>O<sub>4</sub>, C@Fe<sub>3</sub>O<sub>4</sub> and Acac-C@Fe<sub>3</sub>O<sub>4</sub>.

### Optimization of pre-concentration conditions

**Effect of pH.** Acidity of a solution shows strong influence on the adsorption capacity of the adsorbent. To detect influence of the acidity of a solution, Pb<sup>2+</sup> was used as the target ion, and the absorbing process was performed at 25 °C for about 20 minutes. The pH of the solution was set in a range from 2.0 and 10.0, and concentrations and amounts of solutions were given at 20 mg L<sup>-1</sup> and 25.0 mL in turn with the same amounts of sorbent. The relevant results are shown in Fig. 6a. The curves obviously indicated the absorptivity of C@Fe<sub>3</sub>O<sub>4</sub> was more than Fe<sub>3</sub>O<sub>4</sub> microsphere in a set range and this may be due to the porous structure of the carbon layer where there are rich oxygenic groups on the surface. The absorptivity of Acac-C@Fe<sub>3</sub>O<sub>4</sub> was higher than C@Fe<sub>3</sub>O<sub>4</sub>. The absorptivity of Acac-C@Fe<sub>3</sub>O<sub>4</sub> was raised from 25% to 90% with pH values from 2.0 to 6.0 and it slightly declined when the pH changed from 6.0 to 9.0 so the absorptivity was obviously decreased with a pH beyond 9.0. The above indicated that the proper pH range should be controlled between 6.0 and 9.0 for better performance of the adsorbent. Compared with the three curves, the result should be attributed to Acac modified on the surface of C@Fe<sub>3</sub>O<sub>4</sub> composites. Acac has convertible enolyl and dicarbonyl structures with the change in acidity. It is beneficial to resist acidity, which helps to form coordination with lead ions.<sup>21</sup> However, the maximum absorptivity of Fe<sub>3</sub>O<sub>4</sub> and C@Fe<sub>3</sub>O<sub>4</sub>

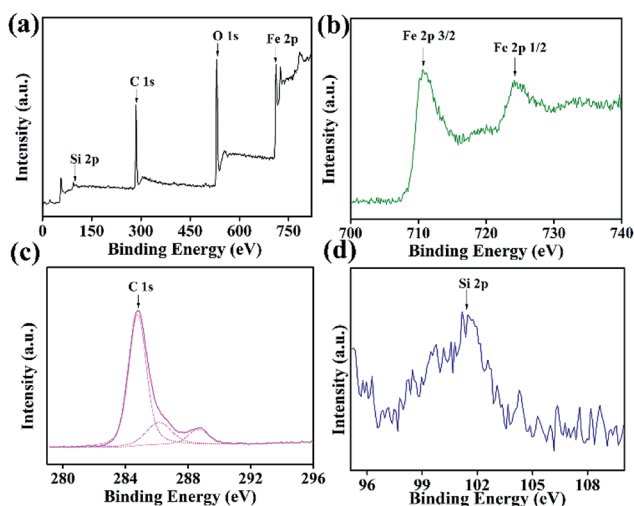


Fig. 3 XPS spectra of Acac-C@Fe<sub>3</sub>O<sub>4</sub>.

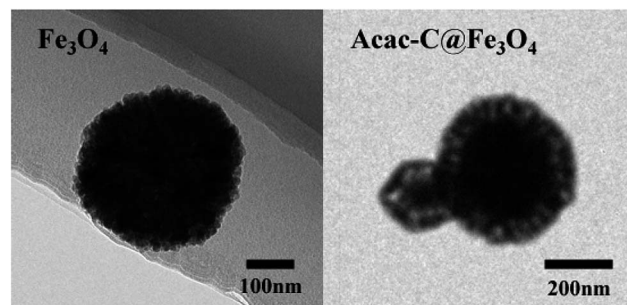


Fig. 5 TEM images of Fe<sub>3</sub>O<sub>4</sub> and Acac-C@Fe<sub>3</sub>O<sub>4</sub>.



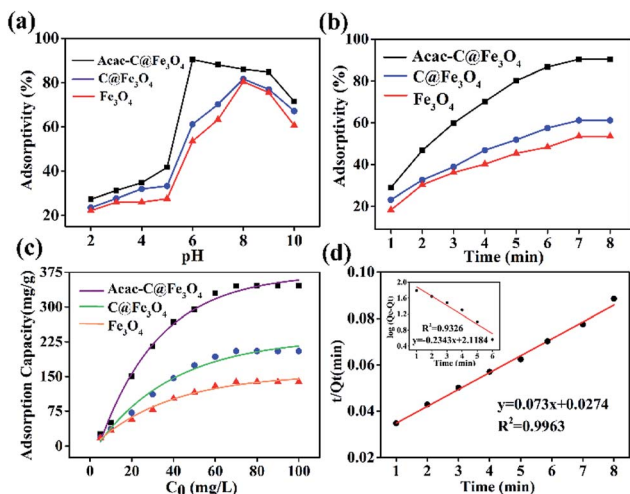


Fig. 6 Effect of pH (a), adsorption time (b), and initial concentration of  $\text{Pb}^{2+}$  (c) on the adsorption of  $\text{Pb}^{2+}$  onto Acac-C@ $\text{Fe}_3\text{O}_4$ , C@ $\text{Fe}_3\text{O}_4$  and  $\text{Fe}_3\text{O}_4$ ; (d) pseudo-second-order kinetic model for  $\text{Pb}^{2+}$  adsorption on Acac-C@ $\text{Fe}_3\text{O}_4$  sorbent (inset: pseudo-first-order kinetic model curve).

microspheres *ca.* 80% appeared at an acidity around 8.0. Since  $\text{Pb}^{2+}$  ions can precipitate under basic conditions, this cannot indicate the as-prepared  $\text{Fe}_3\text{O}_4$  microsphere are a suitable lead ion adsorbent although the adsorption capacity is higher in an alkaline setting.

**Effect of adsorption time.** Adsorption time is an important factor in the application of the as-prepared sorbent. Fig. 6b demonstrates the results about adsorptivity *versus* absorbing time at given conditions including the pH at 6.0, temperature at 25 °C and concentration of  $\text{Pb}^{2+}$  at 20  $\text{mg L}^{-1}$ . These three curves indicated that the adsorptivity increased rapidly within 7 min but after that it remained almost unchanged. The adsorption equilibrium of the absorbing system was reached after around 7 minutes, which suggests the Acac-C@ $\text{Fe}_3\text{O}_4$  adsorbent can achieve the maximum adsorption efficiency within 7 minutes in the testing system, and the adsorption rate of lead ions under the conditions investigated was more than 90%. Relatively, the adsorption rate of lead ions was 61% absorbed by the C@ $\text{Fe}_3\text{O}_4$  microsphere and only 54% by naked  $\text{Fe}_3\text{O}_4$  at same time. The above indicated that the as-prepared Acac-C@ $\text{Fe}_3\text{O}_4$  adsorbent had excellent capacity for lead ions, so it could reach the absorption equilibrium quickly. It is beneficial to use the sorbent in the field of separation of heavy metal ions. As the initial concentration of lead ions was raised, the adsorption amount of Acac-C@ $\text{Fe}_3\text{O}_4$  sorbent also increased gradually and reached to a maximum value greater than 345.3  $\text{mg g}^{-1}$  with a lead ion concentration at 70  $\text{mg L}^{-1}$ , thus basically remaining unchanged. Meanwhile, the adsorption capacity of C@ $\text{Fe}_3\text{O}_4$  and  $\text{Fe}_3\text{O}_4$  microspheres only reached 205.0  $\text{mg g}^{-1}$  and 138.4  $\text{mg g}^{-1}$ , respectively. The maximum adsorption amount of Acac-C@ $\text{Fe}_3\text{O}_4$  was obviously higher than C@ $\text{Fe}_3\text{O}_4$  and the naked  $\text{Fe}_3\text{O}_4$  compared to the three curves. This indicated the saturated adsorption capacity of Acac-C@ $\text{Fe}_3\text{O}_4$  can be acquired with a lead ion concentration beyond

70.0  $\text{mg L}^{-1}$ . Because all available adsorption sites of as-prepared adsorbent were occupied by ions in a high concentration ion solution, it cannot achieve more amounts of ionic adsorption.<sup>31</sup> This suggested the absorption process should belong to chemical absorption.

**Adsorption kinetics study.** An adsorption isotherm expresses the relationship between adsorption capacity and time equilibrium. The experimental data were obtained by detecting the absorbing amount with a series of given absorbing times with the concentration of  $\text{Pb}^{2+}$  ions at 70  $\text{mg L}^{-1}$ . The corresponding data were calculated according to two Langmuir isotherm model formula including pseudo-first-order (1) and pseudo-second-order eqn (2):<sup>32</sup>

$$\log(Q_e - Q_t) = \log Q_e - k_1 t / 2.303 \quad (1)$$

$$\frac{t}{Q_t} = \frac{1}{k_2 Q_e^2} + \frac{t}{Q_e} \quad (2)$$

where  $Q_e$  and  $Q_t$  refer to the adsorption amount of  $\text{Pb}^{2+}$  at equilibrium and time  $t$ , respectively, and  $k_1$ ,  $k_2$  are the rate constants of pseudo-first-order and pseudo-second-order.

According to the model formula, two linear fitting curves and equations are separately shown in Fig. 6d. The analysis results suggested that the pseudo-second-order model ( $R^2 = 0.9915$ ) provided a better description of the  $\text{Pb}^{2+}$  adsorption isotherm process than the pseudo-first-order model based on the fitted correlation coefficients ( $R^2$ ) 0.996 for the second order and 0.933 for the first order model. These results further suggested the absorbing process belongs to a chemical process.

**Adsorption of other heavy metal ions.** Due to Acac having a strong coordination capacity with many metal ions, the sorption capacity of the as-prepared adsorbent for various common metal ions ( $\text{Hg}^{2+}$ ,  $\text{Cr}^{3+}$ ,  $\text{Fe}^{2+}$ ,  $\text{Cd}^{2+}$ ,  $\text{Mn}^{2+}$ ,  $\text{Zn}^{2+}$  and  $\text{Cu}^{2+}$ ) were investigated in parallel under the same conditions. The concentration of all them was given at 70  $\text{mg L}^{-1}$  with the same optimal conditions as the  $\text{Pb}^{2+}$  adsorbing procedures. All data are shown in Fig. 7. This showed that the absorbing capacities of the Acac-C@ $\text{Fe}_3\text{O}_4$  sorbent on  $\text{Hg}^{2+}$ ,  $\text{Cr}^{3+}$ ,  $\text{Fe}^{2+}$ ,  $\text{Cd}^{2+}$ ,  $\text{Mn}^{2+}$ ,  $\text{Zn}^{2+}$  and  $\text{Cu}^{2+}$  were 98.0, 151.2, 189.9, 202.2, 286.3, 297.2 and 305.1  $\text{mg g}^{-1}$ , respectively. These results illustrated that the Acac-C@ $\text{Fe}_3\text{O}_4$  composites can be applied as a highly efficient sorbent for absorbing some common metal ions, which was beneficial for enriching some metal ions in aqueous solution. In order to measure the quality of the prepared adsorbents, saturated adsorbents were compared with some reported metal ion adsorbents and are shown in Table 1. These data indicated that the as-prepared Acac-C@ $\text{Fe}_3\text{O}_4$  adsorbent presented outstanding advantages in adsorption capacity which should be attributed to the functionalization of  $\text{Fe}_3\text{O}_4$  microspheres by Acac and carbon.

## Regeneration of the sorbent

**Selection of a desorption solution.** Regeneration property and method are important parameters to evaluate an adsorbent. Regeneration of the Acac-C@ $\text{Fe}_3\text{O}_4$  composite materials was investigated. First, the type of desorption solution was



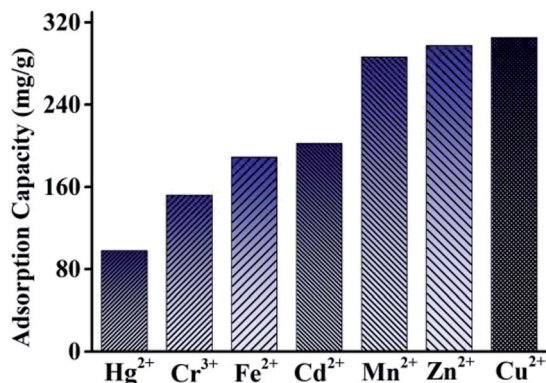


Fig. 7 The adsorption capacity of the as-prepared sorbent for other heavy metal ions.

selected from four kind of common solutions ( $\text{H}_2\text{SO}_4$ ,  $\text{HNO}_3$  and  $\text{HCl}$  at  $1 \text{ mol L}^{-1}$  and  $\text{EDTA}$  at  $0.5 \text{ mol L}^{-1}$ ). They were used to desorb  $\text{Pb}^{2+}$  from the magnetic sorbent and the desorption efficiencies of them are shown in Fig. 8a. This proved that a  $\text{HCl}$  solution was the most suitable for use for desorption because it had the highest effective desorption among those tested. On this basis, the influence of the concentration of a  $\text{HCl}$  solution was further explored and the data are shown in Fig. 8a. With an increase of the  $\text{HCl}$  concentration desorption efficiency increased as the solution concentration changed from  $0.2$  to  $2.0 \text{ mol L}^{-1}$ , and then the desorption efficiency decreased slightly. The above results indicated that desorption solution acidity was an important factor for desorbing lead ion from the as-prepared magnetic sorbent. The coordination sites with  $\text{Pb}^{2+}$  were more and more occupied by  $\text{H}^+$  with increased concentration of the  $\text{HCl}$  solution, so high acidity was an advantage to regenerate the sorbent. However, when concentration of desorption solution was beyond  $2.0 \text{ mol L}^{-1}$ , the desorption performance could keep a high level, but the colour of the desorption solution changed to pale yellow, which might be due to  $\text{Fe}^{3+}$  ion being generated and suggesting that  $\text{Acac-C@Fe}_3\text{O}_4$  materials were damaged in a high acidic setting. So, the concentration of the  $\text{HCl}$  solution used as a desorption solution should be controlled between  $1.0$  and  $2.0 \text{ mol L}^{-1}$  when desorption efficiency of  $\text{Acac-C@Fe}_3\text{O}_4$  sorbent is beyond  $95\%$ .

Meanwhile, the effects of  $\text{HCl}$  solution volume and desorption time on desorption were also studied. The desorbed efficiency was obviously raised with the increase of  $\text{HCl}$  solution volume under  $50.0 \text{ mL}$  as shown in Fig. 8b. There was no change

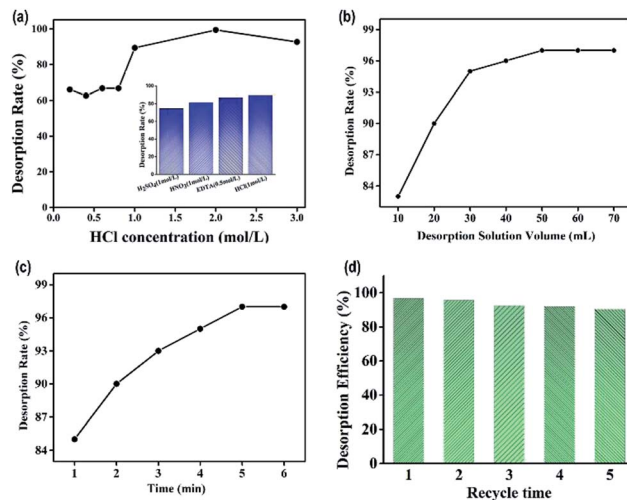


Fig. 8 (a) Influence of the concentration of  $\text{HCl}$  solution and the kind of desorption solution (inset) on the desorption efficiency; the influence of desorption solution volume (b) and desorption time (c) on the desorption efficiency; (d) desorption and regeneration of the as-prepared sorbent.

when the volume was more than  $50.0 \text{ mL}$ . Hence,  $50.0 \text{ mL}$  desorption solution was used in subsequent research. The desorbed time also affects the desorption process. Fig. 8c showed the recovery of the lead ions was up to  $97\%$  when the desorbed time was  $5 \text{ min}$ . And then, the desorption efficiency kept stable even if time was increased. So we choose  $5 \text{ min}$  as optimum desorption.

**Reuse studies.** The reusability of a sorbent is crucial in practical applications. Fig. 8d indicated the results from five time's consecutive adsorption–desorption cycles of  $\text{Pb}^{2+}$  on the  $\text{Acac-C@Fe}_3\text{O}_4$  microspheres. The desorption efficiency still maintained beyond  $90\%$  after 5 times which clearly indicated that absorption capacity just decreased slightly and this decrease of sorption efficiency may be ascribed to loss of adsorbents in a recycled application. The above experimental results suggest our as-prepared  $\text{Acac-C@Fe}_3\text{O}_4$  microspheres sorbent possess fine reusability.

## Conclusions

An  $\text{Acac-C@Fe}_3\text{O}_4$  magnetic adsorbent was successfully prepared by a simple and sustainable procedure and its structure and properties were detected *via* numerous instrumental

Table 1 Comparison of the adsorption capacities of different adsorbents for the removal of heavy metal ions

Adsorbent	Adsorption capacity of metal ions ( $\text{mg g}^{-1}$ )							$\text{Pb}^{2+}$	Ref.
	$\text{Hg}^{2+}$	$\text{Cr}^{3+}$	$\text{Fe}^{2+}$	$\text{Cd}^{2+}$	$\text{Mn}^{2+}$	$\text{Zn}^{2+}$	$\text{Cu}^{2+}$		
$\text{Acac-C@Fe}_3\text{O}_4$	98.0	151.2	188.9	202.2	286.3	297.2	305.1	345.3	This work
PEI-magnetic porous	—	—	—	105.2	—	138.8	157.8	—	33
$\text{Fe}_3\text{O}_4\text{-C-SO}_3\text{H/-COOH}$	83.1	—	—	39.7	—	—	—	90.7	20
$\text{Fe}_3\text{O}_4\text{-APS@AA-co-CA}$	—	—	—	29.6	—	43.4	126.9	166.1	34
Magnetic PSSQ hybrid	—	—	—	5.2	13.3	—	30.0	66.1	35
$\text{Poly(MMA-co-MA)/Fe}_3\text{O}_4$	—	90.91	—	—	—	111.11	109.89	—	36
Coir fibers	—	—	11.11	—	—	—	9.43	24.91	37





measurements. The adsorbent demonstrated outstanding adsorption capacity for some metal ions. Under given conditions, the maximum adsorption capacities for  $\text{Hg}^{2+}$ ,  $\text{Cr}^{3+}$ ,  $\text{Fe}^{2+}$ ,  $\text{Cd}^{2+}$ ,  $\text{Mn}^{2+}$ ,  $\text{Zn}^{2+}$ ,  $\text{Cu}^{2+}$  and  $\text{Pb}^{2+}$  were 98.0, 151.2, 188.9, 202.2, 286.3, 297.2, 335.1 and 345.3  $\text{mg g}^{-1}$ , respectively. The adsorption process reached adsorption equilibrium within 7 min and conforms to a pseudo-second-order kinetics model. The adsorbent had excellent stability and reusability. The  $\text{Acac-C@Fe}_3\text{O}_4$  magnetic adsorbent may provide an alternative for applications in the adsorption and separation of heavy metal ions in aqueous solutions. What's more, the material can be used as a substrate and in the further synthesis of metal-organic frameworks.

## Conflicts of interest

There are no conflicts to declare.

## Acknowledgements

This work was financially supported by the Natural Science Foundation of Shanghai (No. 15ZR1428500) and the National Natural Science Foundation of China (No. 20906061).

## Notes and references

- 1 Z. S. Kardar, M. H. Beyki and F. Shemirani, Takovite-aluminosilicate@ $\text{MnFe}_2\text{O}_4$  nanocomposite, a novel magnetic sorbent for efficient preconcentration of lead ions in food samples, *Food Chem.*, 2016, **209**, 241–247.
- 2 F. L. Fu and Q. Wang, Removal of heavy metal ions from wastewaters: a review, *J. Environ. Manage.*, 2011, **92**(3), 407–418.
- 3 F. R. Peligro, I. Pavlovic, R. Rojas and C. Barriga, Removal of heavy metals from simulated wastewater by *in situ* formation of layered double hydroxides, *Chem. Eng. J.*, 2016, **336**, 1035–1040.
- 4 H. Wang, F. Chen, S. Mu, D. Zhang, X. Pan, D. J. Lee and J. S. Chang, Removal of antimony (Sb (V)) from Sb mine drainage: biological sulfate reduction and sulfide oxidation-precipitation, *Bioresour. Technol.*, 2013, **146**, 799–802.
- 5 F. Fu, L. Xie, B. Tang, Q. Wang and S. Jiang, Application of a novel strategy—Advanced Fenton-chemical precipitation to the treatment of strong stability chelated heavy metal containing wastewater, *Chem. Eng. J.*, 2012, **189**, 283–287.
- 6 S. J. Kim, K. H. Lim, K. H. Joo, M. J. Lee, S. G. Kil and S. Y. Cho, Removal of heavy metal-cyanide complexes by ion exchange, *Korean J. Chem. Eng.*, 2002, **19**(6), 1078–1084.
- 7 X. Li, G. M. Zeng, J. H. Huang, C. Zhang, Y. Y. Fang, Y. H. Qu, F. Luo, D. Lin and H. L. Liu, Recovery and reuse of surfactant SDS from a MEUF retentate containing  $\text{Cd}^{2+}$  or  $\text{Zn}^{2+}$  by ultrafiltration, *J. Membr. Sci.*, 2009, **337**(1–2), 92–97.
- 8 C. M. Zhong, Z. L. Xu, X. H. Fang and L. Cheng, Treatment of acid mine drainage (AMD) by ultra-low-pressure reverse osmosis and nanofiltration, *Environ. Eng. Sci.*, 2007, **24**(9), 1297–1336.
- 9 K. I. Dermentzis, A. E. Davidis, A. S. Dermentzi and C. D. Chatzichristou, An electrostatic shielding-based coupled electrodialysis/electrodeionization process for removal of cobalt ions from aqueous solutions, *Water Sci. Technol.*, 2010, **62**(8), 1947–1953.
- 10 C. Y. Teh, P. M. Budiman, K. P. Y. Shak and T. Y. Wu, Recent advancement of coagulation-flocculation and its application in wastewater treatment, *Ind. Eng. Chem. Res.*, 2016, **55**(16), 4363–4389.
- 11 H. Polat and D. Erdogan, Heavy metal removal from waste waters by ion flotation, *J. Hazard. Mater.*, 2007, **148**(1–2), 267–273.
- 12 T. K. Tran, H. J. Leu, K. F. Chiu and C. Y. Lin, Electrochemical Treatment of Heavy Metal-containing Wastewater with the Removal of COD and Heavy Metal Ions, *J. Chin. Chem. Soc.*, 2017, **64**(5), 493–502.
- 13 H. B. Bradl, Adsorption of heavy metal ions on soils and soils constituents, *J. Colloid Interface Sci.*, 2004, **277**(1), 1–18.
- 14 X. Li, S. F. Wang, Y. G. Liu, L. H. Jiang, B. Song, M. F. Li, G. M. Zeng, X. F. Tan, X. X. Cai and Y. Ding, Adsorption of Cu (II), Pb (II), and Cd (II) ions from acidic aqueous solutions by diethylenetriamine- pentaacetic acid-modified magnetic graphene oxide, *J. Chem. Eng. Data*, 2016, **62**(1), 407–416.
- 15 M. Hua, S. J. Zhang, B. C. Pan, W. M. Zhang, L. Lv and Q. X. Zhang, Heavy metal removal from water/wastewater by nanosized metal oxides: a review, *J. Hazard. Mater.*, 2012, **211**, 317–331.
- 16 Y. L. Wang, X. Zhang, L. Gao, Y. Mao, X. Hu and W. D. Lou, One-Pot Magnetic Field Induced Formation of  $\text{Fe}_3\text{O}_4/\text{C}$  Composite Microrods with Enhanced Lithium Storage Capability, *Small*, 2014, **10**(14), 2815–2819.
- 17 Y. L. Wang, Y. Zhang, Y. Wu, Y. Zhong, X. Hu and W. D. Lou, Carbon-coated  $\text{Fe}_3\text{O}_4$  microspheres with a porous multideck-cage structure for highly reversible lithium storage, *Chem. Commun.*, 2015, **51**(32), 6921–6924.
- 18 Y. Liu, L. Zhou, Y. Hu, C. Guo, H. Qian, F. X. Zhang and W. D. Lou, Magnetic-field induced formation of 1D  $\text{Fe}_3\text{O}_4/\text{C}/\text{CdS}$  coaxial nanochains as highly efficient and reusable photocatalysts for water treatment, *J. Mater. Chem.*, 2011, **21**(45), 18359–18364.
- 19 M. Bystrzejewski, K. Pyrzyńska, A. Huczko and H. Lange, Carbon-encapsulated magnetic nanoparticles as separable and mobile sorbents of heavy metal ions from aqueous solutions, *Carbon*, 2009, **47**(4), 1201–1204.
- 20 Z. Chen, Z. Geng, Z. Zhang, L. b. Ren, T. T. Tao, R. C. Yang and Z. X. Guo, Synthesis of magnetic  $\text{Fe}_3\text{O}_4/\text{C}$  nanoparticles modified with  $-\text{SO}_3\text{H}$  and  $-\text{COOH}$  groups for fast removal of  $\text{Pb}^{2+}$ ,  $\text{Hg}^{2+}$ , and  $\text{Cd}^{2+}$  ions, *Eur. J. Inorg. Chem.*, 2014, (20), 3172–3177.
- 21 M. H. Xu, J. Chai, N. T. Hu, D. Huang, Y. X. Wang, X. L. Huang, H. Wei, Z. Yang and Y. F. Zhang, Facile synthesis of soluble functional graphene by reduction of graphene oxide *via* acetylacetone and its adsorption of heavy metal ions, *Nanotechnology*, 2014, **25**(39), 395602.
- 22 S. H. Liu, R. M. Xing, F. Lu, R. K. Rana and J. J. Zhu, One-pot template-free fabrication of hollow magnetite nanospheres



- and their application as potential drug carriers, *J. Phys. Chem. C*, 2009, **113**(50), 21042–21047.
- 23 X. Y. Zhang, S. C. Zhu, C. H. Deng and X. M. Zhang, Highly sensitive thrombin detection by matrix assisted laser desorption ionization-time of flight mass spectrometry with aptamer functionalized core-shell  $\text{Fe}_3\text{O}_4@\text{C}@\text{Au}$  magnetic microspheres, *Talanta*, 2012, **88**, 295–332.
  - 24 Q. H. Li, X. Z. Ren, L. Z. Tong, X. D. Chen, H. Ding and H. Yang, Deposition of luminescence  $\text{YBO}_3:\text{Eu}^{3+}, \text{Gd}^{3+}$  on ferromagnetic  $\text{Fe}@\text{C}$  nanoparticles, *Dyes Pigm.*, 2014, **107**, 161–165.
  - 25 X. F. Lu, H. Mao, D. M. Chao, W. J. Zhang and Y. Wei, Ultrasonic synthesis of polyaniline nanotubes containing  $\text{Fe}_3\text{O}_4$  nanoparticles, *J. Solid State Chem.*, 2006, **179**(8), 2609–2615.
  - 26 Z. Y. Zhang and J. L. Kong, Novel magnetic  $\text{Fe}_3\text{O}_4@\text{C}$  nanoparticles as sorbents for removal of organic dyes from aqueous solution, *J. Hazard. Mater.*, 2011, **193**, 325–329.
  - 27 J. R. Meng, C. Y. Shi, B. W. Wei, W. J. Yu, C. H. Deng and X. M. Zhang, Preparation of  $\text{Fe}_3\text{O}_4@\text{C}@\text{PANI}$  magnetic microspheres for the extraction and analysis of phenolic compounds in water samples by gas chromatography–mass spectrometry, *J. Chromatogr. A*, 2011, **1218**(20), 2841–2847.
  - 28 S. K. Li, F. Z. Huang, Y. Wang, Y. H. Shen, L. G. Qiu, A. J. Xie and S. J. Xu, Magnetic  $\text{Fe}_3\text{O}_4@\text{C}@\text{Cu}_2\text{O}$  composites with bean-like core/shell nanostructures: synthesis, properties and application in recyclable photocatalytic degradation of dye pollutants, *J. Mater. Chem.*, 2011, **21**(20), 7459–7466.
  - 29 D. Saberi, S. Mahdudi, S. Cheraghi and A. Heydari,  $\text{Cu}(\text{II})$ –acetylacetone complex covalently anchored onto magnetic nanoparticles: Synthesis, characterization and catalytic evaluation in amide bond formation *via* oxidative coupling of carboxylic acids with N, N-dialkylformamides, *J. Organomet. Chem.*, 2014, **772**, 222–228.
  - 30 C. Guo, W. Lu, G. Wei, L. Jiang, Y. Yu and Y. Hu, Formation of 1D chain-like  $\text{Fe}_3\text{O}_4@\text{C}/\text{Pt}$  sandwich nanocomposites and their magnetically recyclable catalytic property, *Appl. Surf. Sci.*, 2018, **457**, 1136–1141.
  - 31 K. Wang, J. W. Gu and N. Yin, Efficient Removal of  $\text{Pb}(\text{II})$  and  $\text{Cd}(\text{II})$  Using  $\text{NH}_2$ -Functionalized Zr-MOFs *via* Rapid Microwave-Promoted Synthesis, *Ind. Eng. Chem. Res.*, 2017, **56**(7), 1880–1887.
  - 32 G. X. Chen, C. D. Qiao, Y. Wang and J. S. Yao, Synthesis of magnetic gelatin and its adsorption property for  $\text{Cr}(\text{VI})$ , *Ind. Eng. Chem. Res.*, 2014, **53**(40), 15576–15581.
  - 33 Y. Pang, G. Zeng, L. Tang, Y. Zhang, Y. Y. Liu, X. X. Lei, Z. Li, J. C. Zhang and G. X. Xie, PEI-grafted magnetic porous powder for highly effective adsorption of heavy metal ions, *Desalination*, 2011, **281**, 278–284.
  - 34 F. Ge, M. M. Li, H. Ye and B. X. Zhao, Effective removal of heavy metal ions  $\text{Cd}^{2+}$ ,  $\text{Zn}^{2+}$ ,  $\text{Pb}^{2+}$ ,  $\text{Cu}^{2+}$  from aqueous solution by polymer-modified magnetic nanoparticles, *J. Hazard. Mater.*, 2012, **211**, 366–372.
  - 35 S. Nagappan, H. M. Ha, S. S. Park, N. J. Jo and C. S. Ha, One-pot synthesis of multi-functional magnetite–polysilsesquioxane hybrid nanoparticles for the selective  $\text{Fe}^{3+}$  and some heavy metal ions adsorption, *RSC Adv.*, 2017, **7**(31), 19106–19116.
  - 36 A. Masoumi, M. Ghaemy and A. N. Bakht, Removal of metal ions from water using poly (MMA-co-MA)/modified- $\text{Fe}_3\text{O}_4$  magnetic nanocomposite: isotherm and kinetic study, *Ind. Eng. Chem. Res.*, 2014, **53**(19), 8188–8197.
  - 37 P. M. Shukla and S. R. Shukla, Biosorption of  $\text{Cu}(\text{II})$ ,  $\text{Pb}(\text{II})$ ,  $\text{Ni}(\text{II})$ , and  $\text{Fe}(\text{II})$  on alkali treated coir fibers, *Sep. Sci. Technol.*, 2013, **48**(3), 421–428.

